

## An objective real-time data-adaptive technique for efficient model resolution improvement in magnetotelluric studies

Alan G. Jones\* and John H. Foster‡

### ABSTRACT

A scheme is described whereby the error associated with the least well-resolved model eigenparameter in a magnetotelluric survey is reduced by focusing data collection on a specific range of frequencies. The scheme also gives a quantitative estimate of the statistical error associated with the least well-resolved model parameter, and thus provides an objective criterion to the operator regarding when to cease data collection at that location.

The scheme is based on a linearization of the relationship between variations in the model parameters and the changes thereby introduced to the computed response function. The matrix of partial derivatives describing this linearization is factored orthogonally by a singular value decomposition.

The scheme is illustrated by applying it to a synthetic data set. Also, the algorithm has been coded in Basic on an HP9845 and employed in the field. An example is given of its field operation in a sedimentary basin environment.

### INTRODUCTION

The operator of a magnetotelluric (MT) survey in any locale is beset with the traditional tradeoff problem of acquiring either highly precise data (i.e., with small standard errors associated with the estimated response functions) at a few sites, or "sufficiently" precise data at many sites. There is to date no in-field objective criterion for defining "sufficient," and it is highly likely that terminating data collection too soon would result in an unacceptable lack of resolution of some of the parameters describing the conductivity-depth structure below the site. Also, for systems that scan frequencies individually, it is inefficient to reduce the standard errors of the MT response functions at all available frequencies when reducing the standard errors at a certain critical range of frequencies performs the same reduction in the standard error of the previously unresolved model parameters.

A scheme is described whereby resolution of the least well-resolved model parameter (or combination of model parameters) is improved by focusing data collection at certain crucial frequencies in order to reduce the standard errors of the response functions at those frequencies. The scheme also gives a quantitative estimate of the standard error associated with the model parameter which is the least well-resolved, and thus gives an objective criterion to the operator as to when to cease data collection at that location.

The scheme is based on a linearization of the relationship between variations in the model parameters and the changes thereby introduced on the theoretically observed response function. The matrix of partial derivatives, or "system matrix," describing the linearization is factored orthogonally by a singular value decomposition (SVD).

The scheme is illustrated by applying it to both a synthetic data set and to a field data set.

### THEORETICAL DETAILS

The theoretical approach used is based on the well-known SVD of the system matrix relating the model parameters to the observations. This approach has been used successfully in solving the one-dimensional (1-D) and two-dimensional (2-D) inverse problems posed by the MT method (Jupp and Vozoff, 1975, 1977a, b; Vozoff and Jupp, 1975; Edwards et al., 1981; Jones, 1982; Cavaliere and Jones, 1984) and in experiment design (Vozoff and Jupp, 1977; Ilkiskik and Jones, 1984). The above articles give a complete discussion on SVD, as do Wiggins (1972) and Lawson and Hanson (1974).

Briefly, for a set of model parameters,  $p_j$ ,  $j = 1, \dots, n$ , which parameterize the conductivity-depth distribution below a location and given observations  $o_i$ ,  $i = 1, \dots, m$ , there exists a highly nonlinear relationship between the two,

$$\mathbf{o} = F(\mathbf{p}). \quad (1)$$

For infinitesimally small order changes in the parameters  $\Delta p_j$  causing small-order changes in the observations  $\Delta o_i$ , then by neglecting terms higher than first order in the Taylor series expansion, an equation relating  $\Delta p_j$  to  $\Delta o_i$  may be written,

Presented at the 53rd Annual International Meeting and Exposition of the Society of Exploration Geophysicists, September 11, 1983, Las Vegas. Manuscript received by the Editor June 4, 1984; revised manuscript received June 21, 1985.

\*Formerly Geophysics Laboratory, Physics Department, University of Toronto, Toronto, Ontario, Canada, M5S 1A7; presently Division of Seismology and Geomagnetism, Earth Physics Branch, Energy, Mines & Resources, Ottawa, Ontario, Canada K1A 0Y3.

‡Phoenix Geophysics Ltd., 200 Yorkland Blvd., Willowdale, Ontario, Canada, M2J 1R5.

© 1986 Society of Exploration Geophysicists. All rights reserved.

$$\Delta \mathbf{o} = \mathbf{A} \Delta \mathbf{p}, \quad (2)$$

where  $\mathbf{A}$  is the matrix of partial derivatives of  $m$  rows and  $n$  columns, consisting of terms of the form

$$a_{ij} = \frac{\partial o_i}{\partial p_j}. \quad (3)$$

The  $m \times n$  matrix  $\mathbf{A}$  can be factored by an SVD into an  $m \times n$  orthonormal matrix  $\mathbf{U}$ , an  $n \times n$  orthonormal matrix  $\mathbf{V}$ , and an  $n \times n$  diagonal matrix  $\mathbf{\Lambda}$  such that

$$\mathbf{A} = \mathbf{U} \mathbf{\Lambda} \mathbf{V}^T \quad (4)$$

(Lanczos, 1961), where  $T$  indicates transpose. The diagonal of  $\mathbf{\Lambda}$  consists of the ordered singular values,  $\lambda_j, j = 1, \dots, n$ , and are such that  $\lambda_1 \geq \lambda_2 \geq \dots \geq \lambda_n$ .  $\mathbf{U}$  contains  $n$  eigenvectors of length  $m$  associated with the columns (observations) of  $\mathbf{A}$  (they are the eigenvectors of  $\mathbf{A} \mathbf{A}^T$ ) while  $\mathbf{V}$  contains  $n$  eigenvectors of length  $n$  associated with the rows (parameters) of  $\mathbf{A}$  (they are the eigenvectors of  $\mathbf{A}^T \mathbf{A}$ ). Rewriting equation (2) in terms of an SVD of matrix  $\mathbf{A}$  gives

$$\Delta \mathbf{o} = \mathbf{U} \mathbf{\Lambda} \mathbf{V}^T \Delta \mathbf{p}, \quad (5)$$

hence

$$(\mathbf{U}^T \Delta \mathbf{o}) = \mathbf{\Lambda} (\mathbf{V}^T \Delta \mathbf{p}), \quad (6)$$

or

$$\Delta \mathbf{o}' = \mathbf{\Lambda} \Delta \mathbf{p}'; \quad (7)$$

and thus the complicated relationship described by equation (2) has been reduced to a linear relationship between "eigen-data," given by

$$\mathbf{o}' = \mathbf{U}^T \mathbf{o}, \quad (8)$$

and "eigenparameters," given by

$$\mathbf{p}' = \mathbf{V}^T \mathbf{p}. \quad (9)$$

Obviously, the first element in  $\mathbf{p}'$ ,  $p'_1$ , is the most sensitive combination of model parameters because small variations in  $p'_1$ , i.e.,  $\Delta p_1$ , result in the largest changes in the observations  $\Delta o'_1$ , because  $\lambda_1$  is the maximum singular value. Conversely, the last element in  $\mathbf{p}'$ ,  $p'_n$ , is the least sensitive eigenparameter. Assuming equation (2) has already been scaled to reflect the standard errors associated with each observation  $o_i$ , then to resolve  $p'_n$  better, it is necessary to reduce the standard errors associated with  $o'_n$ . From equation (8),  $o'_n$  is given by a linear combination of the observations  $\mathbf{o}$ , and that linear combination is detailed by the last row of  $\mathbf{U}^T$ , i.e., the last column of  $\mathbf{U}$ ,

$$o'_n = \sum_{i=1}^m u_{in} o_i. \quad (10)$$

Hence, concentrating data collection on those frequencies that have significant contributions in the last column of  $\mathbf{U}$  results in a reduction of the standard errors of the data at those frequencies, and accordingly a superior resolution of  $p'_n$ .

Virtually all previously mentioned works concentrated on which model eigenparameters were best resolved by considering  $\mathbf{V}$ , and were only interested in  $\mathbf{U}$  for information purposes because it was usually assumed data were already available and were not being collected. However, in our approach we are more concerned with  $\mathbf{U}$ , because our data collection is

ongoing and we are undertaking our analysis in real time.

The standard error associated with  $p'_n$ , the worst resolved eigenparameter, is  $1/\lambda_n$ . If this error is less than a certain value previously dictated by the client or party geophysicist, then the operator can, in complete confidence, end data collection and move to a new location. If  $1/\lambda_n$  is greater than this value, however, the operator knows that the standard errors at the frequencies described by the last column of  $\mathbf{U}$  are still too large for adequate resolution of the model parameters to within the required accuracy. Hence, more data need to be collected.

It is important that the model be correctly parameterized; otherwise highly misleading and biased information could result. In order that the layer resistivities  $\rho_j$  and the layer thicknesses  $h_j$  have nondimensional units, and that the system matrix not be biased (for example, by thick layers preferentially over thin ones), the logarithms of these layer parameters are the chosen model parameters. Hence, the model is parameterized in terms of  $(2\ell - 1)$  parameters, where  $\ell$  is the number of layers, and these are  $\log(\rho_j), j = 1, \dots, \ell$  followed by  $\log(h_j), j = 1, \dots, \ell - 1$ . Such a parameterization is also quite natural in electromagnetic induction studies due to the skin depth attenuation effect that exhibits an exponential decay characteristic.

For the observations, this work concentrates solely on the MT apparent resistivity data; the extension to include measured phase data is trivial. It is well-known that the apparent resistivity displays a lognormal distribution rather than a normal one (Bentley, 1973; Fournier and Febrer, 1976); hence, the observations are  $\log[(\rho_a)_i], i = 1, \dots, m$  observed at  $m$  frequencies. Accordingly, the matrix of partial derivatives consists of terms of the form

$$a_{ij} = \frac{\partial \log[(\rho_a)_i]}{\partial \log(p_j)}, \quad (11)$$

where

$$p_j = \begin{cases} \rho_j, & j \leq \ell \\ h_{j-\ell}, & j > \ell \end{cases} \quad (12)$$

Finally, the matrix  $\mathbf{A}$  must be scaled to reflect the differing standard errors associated with each observation. This is accomplished by dividing the elements  $a_{ij}$ , given as equation (11), by the standard errors on a logarithmic scale at each  $j$ th frequency  $e_j$ . For example,  $e_j = 1$  implies that the standard errors of that particular apparent resistivity are plus or minus one decade. Hence, the scaled matrix consists of terms such as

$$a_{ij} = \frac{1}{e_j} \frac{\partial \log[(\rho_a)_i]}{\partial \log(p_j)}. \quad (13)$$

## PRACTICAL DETAILS

To derive the matrix of partial derivatives  $\mathbf{A}$ , a model must be sought which is indicative, to first order, of the conductivity-depth distribution below the location. This inverse problem is certainly nontrivial, and much effort has been expended in this direction in recent years. However, the objective of the proposed scheme is *not* to undertake a comprehensive 1-D in-field inversion of the data, but to identify those frequencies at which the standard errors need to be reduced compared preferentially to other frequencies. Hence, it is suf-

ficient that the model used be representative of the true conductivity-depth structure, and that the two are "linearly-close".

The first-order approximation scheme employed by the authors for deriving a model from the observed response is a slight modification of the well-known Niblett-Bostick transformation (Niblett and Sayn-Wittgenstein, 1960; Bostick, 1977; Jones, 1983). The Niblett-Bostick transformation gives a resistivity  $\rho_B$  at depth  $h$ , from the apparent resistivity curve alone, by

$$h = \left[ \frac{\rho_a(T)T}{2\pi\mu} \right]^{1/2} \quad (14)$$

and

$$\rho_B(h) = \rho_a(T) \left[ \frac{1 + m(T)}{1 - m(T)} \right], \quad (15)$$

where  $T$  is the period of interest and  $m(T)$  is the gradient of the apparent resistivity curve with increasing period in log-log space, i.e.,

$$m(T) = \frac{d \log [\rho_a(T)]}{d \log (T)}. \quad (16)$$

The Niblett-Bostick transform is known to perform well in the case of a decrease in resistivity with depth, but not so well for an increase of resistivity with depth. This is due to the reluctance of current to enter a more resistive layer. To compensate partially for this effect, the gradient of  $m(T)$  can be taken into consideration, i.e.,

$$m'(T) = \frac{d^2 \log [\rho_a(T)]}{d^2 \log (T)}. \quad (17)$$

If both  $m(T)$  and  $m'(T)$  are positive, then the apparent resistivity curve indicates that, at the periods of interest, a transition is being made between a less resistive layer to an underlying more resistive one. Conversely, if both  $m(T)$  and  $m'(T)$  are negative, then the opposite is true. Hence, a first-order inversion is defined by resistivity  $\rho_J$ , at depth  $h$ , given by

$$\rho_J(h) = \rho_a(T) \left[ \frac{1 + m(T)}{1 - m(T)} \right] \quad \text{for sign}(m) \neq \text{sign}(m'), \quad (18)$$

or

$$\rho_J(h) = \rho_a(T) \left[ \frac{1 + \text{sign}(m)(|m|)^q}{1 - \text{sign}(m)(|m|)^q} \right] \quad \text{for sign}(m) = \text{sign}(m'),$$

where

$$q = 1/(1 + m)^2 \quad \text{for } m(T) > 0,$$

or (19)

$$q = 1/(1 - m)^{1/2} \quad \text{for } m(T) < 0.$$

A comparison of a true model with the Niblett-Bostick transformation and the transformation described above of the theoretically observed response is illustrated in Figure 1. As can be seen, the modified transformation gives a sharper increase with depth on entering the lower resistive zone. The continuous model, defined by  $\rho_J(h)$ , is subsequently "blocked" such that each maximum and minimum is considered to define a layer of that resistivity. The interface between two adjacent layers is placed at the depth where  $\rho_J(h)$  displays a resistivity

equal to the geometric mean of the two layer resistivities. Any adjacent layers are then joined together if their layer resistivities differ by less than one-quarter of a decade, ensuring that the total conductivity-thickness product equals the sum of the two individual ones. For the model of interest, the "blocked" first approximation model is as illustrated in Figure 1. Note that the third layer in the blocked model does not have the resistivity given by the maximum value (at a depth of approximately 7 000 m), because the layer defined by this maximum value was joined with the underlying half-space.

The described method could, of course, be replaced by any other method thought to be superior for in-field determination, for example Fischer's analytical algorithm (Fischer et al., 1981). However, the scheme chosen must be computationally fast enough to work in real time without interrupting data collection.

Once a suitable model is discovered, matrix  $\mathbf{A}$  can be derived and factored by an SVD. The operator can then be informed of (1) the value of  $\lambda_n$ , which indicates whether to end data collection or not; (2) the last column of  $\mathbf{Y}$ , which gives the mixed model parameter least resolved; and (3) the last column of  $\mathbf{U}$ , stating which frequencies are crucial for improving the resolution of (2).

## SYNTHETIC EXAMPLE

The theoretical model shown in Figure 1 was used to illustrate the proposed scheme. Geologically, it represents a fractured basalt layer, of resistivity 125  $\Omega \cdot \text{m}$  and thickness 1 500 m, overlying 1 000 m of sediments of 15  $\Omega \cdot \text{m}$ , with a basement of 250  $\Omega \cdot \text{m}$ . The theoretical MT apparent resistivity response observed over this structure in the frequency range  $10^{-2}$  to  $10^2$  Hz is shown in Figure 2. For this example, a sampling of 3 points per decade was chosen to keep the matrices small enough for illustration purposes. However, the scheme can be applied for any sampling.

The matrix of partial derivatives was generated from the derived blocked model, not the true theoretical model (which would be unknown for real data), and subsequently scaled to reflect a standard error of 0.25 (25 percent) on all data (i.e., one-quarter of a decade). An SVD factoring of  $\mathbf{A}$  into the component matrices  $\mathbf{U}$ ,  $\mathbf{\Lambda}$ , and  $\mathbf{V}$  was undertaken, and the matrices were inspected (Figure 3).

As other similar studies have shown for the case of a resistive-conductive-resistive model, the best-resolved model parameter is the conductivity-thickness product of the conducting layer,  $S_2 = \sigma_2 h_2$  (Figure 3a). This is deduced from the fact that the two model parameters with the greatest contribution to the best-resolved eigenparameter  $\rho'_1$  are given by  $\log(\rho_2)$  and  $\log(h_2)$ . However, the contributions are of opposite sign and hence the eigenparameter is equivalent to  $\log(h_2) - \log(\rho_2) = \log(h_2/\rho_2) = \log(S_2)$ . The standard error of  $\log(S_2)$  is less than 0.08. The other reasonably well-resolved parameters and their associated standard errors, in decreasing order of resolution, are:  $\log(T_1)$ , 0.10 (Figure 3b);  $\log(S_1)$ , 0.15 (Figure 3c); and  $\log(\rho_3)$ , 0.30 (Figure 3d). The least resolved parameter is  $\log(T_2)$ , the resistivity-thickness product of the conducting layer, with a standard error greater than 1 (Figure 3e and Figure 4a). The SVD factorization illustrates that the orthogonal parameterization of the second layer is not  $\rho_2$  and  $h_2$  as used, but  $S_2$  and  $T_2$ , the Dar-Zarrouk parameterization

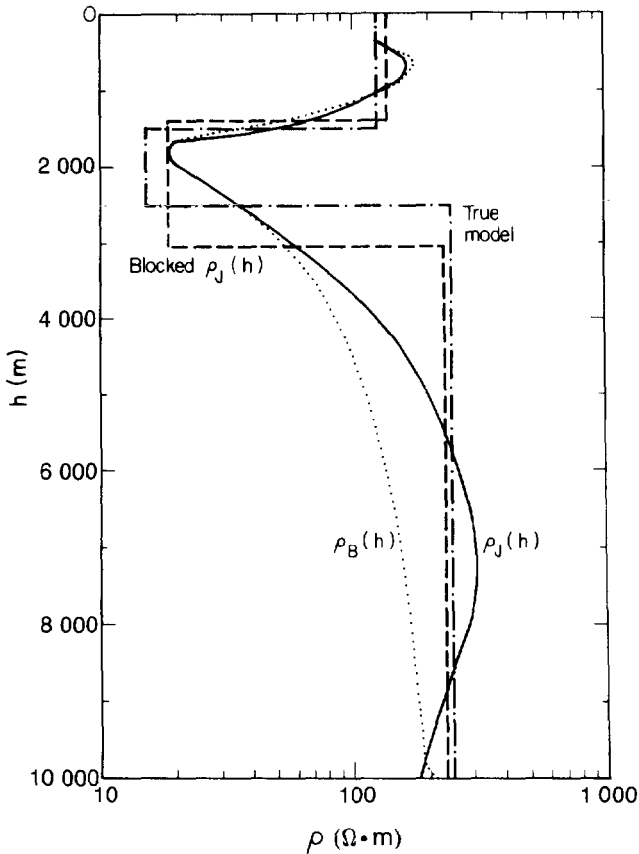


FIG. 1. A comparison of a Niblett-Bostick first-order inverse ( $\rho_B$ , dotted line) and an inverse which takes into consideration the second-order derivative of the apparent resistivity curve ( $\rho_J$ , solid line) with the true resistivity-depth distribution that generated the theoretical response (dashed-dotted line). Also shown is the "blocked" first-order inverse proposed (dashed line).

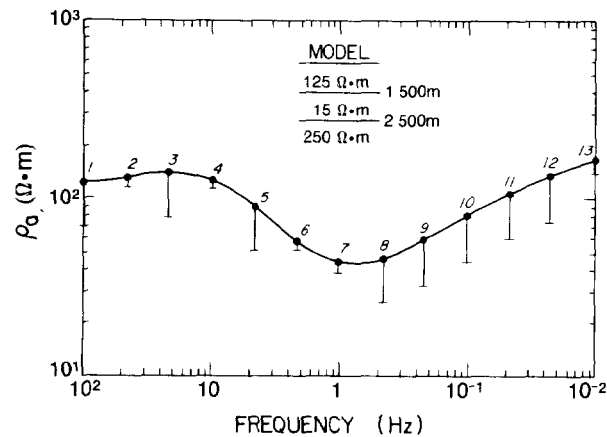


FIG. 2. The theoretical response of the true model shown in Figure 1, with the standard errors of the data points at the conclusion of the synthesized data acquisition.

(Maillet, 1947). Hence although both parameters of the uppermost (basalt) layer are sufficiently well-resolved, the conductivity and thickness of the conducting (sediment) layer are not independently determined; thus no reliable estimate of the depth to basement is possible.

To obtain better resolution of  $T_2$ , it is necessary to reduce the standard errors of those frequencies that have a significant contribution to the last column of the  $\mathbf{U}$  matrix (Figures 3e and 4a). Frequencies 4 (10 Hz), 6 (2.2 Hz), and 7 (1 Hz) (Figure 4a) all have contributions exceeding 10 percent. (The relative contribution of each  $u_{i5}$  is given by its square, since the sum of squares of all elements down any one column of  $\mathbf{U}$ , and  $\mathbf{V}$ , equals unity.) Reducing the standard errors of only those three frequencies from 0.25 to 0.13 (which replicates greater data collection in the field at those frequencies alone) causes a reduction in the standard error of  $\log(T_2)$  from 1.2 to 0.34. The resolution of the other eigenparameters is also improved.

Again, the last column of  $\mathbf{U}$  indicates that frequencies 2 (46 Hz), 4, 6, and 7 need smaller standard errors to improve the resolution of  $T_2$  (Figure 4b). Reducing each of them by one-half (0.25 to 0.13 for frequency 2, 0.13 to 0.06 for the other three frequencies) results in a reduction in the standard error of  $\log(T_2)$  from 0.34 to 0.20. Also, all other model parameters have far smaller associated standard errors.

In the third stage, the last column of  $\mathbf{U}$  is as illustrated in Figure 4c. Frequencies 2, 4, and 13 are identified as being most important for the least-resolved, mixed-model parameter, which is now a combination of  $\rho_2$ ,  $\rho_3$ , and  $h_2$ , or  $T_2\rho_3$ . Frequency 7 no longer plays an important role. Note also that the least-resolved eigenparameter now includes  $\rho_3$  because the lowest frequency (longest period), number 13, is of importance at this stage.

Cycling through and reducing the statistical error of each of the four important frequencies by one-half (i.e., frequency 2 from 13 percent to 6 percent, 4 and 6 from 6 percent to 3 percent, and 13 from 25 percent to 13 percent), results in the last columns of  $\mathbf{U}$  and  $\mathbf{V}$  as shown in Figure 4d. The standard error associated with  $v_5$  is now 1/8.7 which is approximately 11.5 percent, and parameter eigenvector  $v_5$  indicates that eigenparameter  $\rho_3 h_2$  is now the least resolved. The important frequencies for  $v_5$ , as indicated by  $u_5$ , are again 2, 4, 6, and 13. However, at this point the standard errors associated with frequencies 4 and 6 are 3 percent, and the operator may decide that no further improvement in precision is possible; hence he may end data collection at these frequencies.

Concentrating on the remaining two frequencies, i.e., 2 and 13, and reducing their standard errors by one-half (to 3 percent for frequency 2, 6 percent for 13) leads to the situation illustrated in Figure 4e for  $u_5$  and  $v_5$ . At this point the error in the least-resolved eigenparameter, which is  $\rho_3 T_2$ , is 10 percent and the frequencies of importance are 2, 4, and 6. However, all three of these frequencies have standard errors which are at the "limits" of the system (in this example, chosen as 3 percent), and hence no further improvement can be made by concentrating data collection on them. There is the possibility of marginal improvement by reducing the standard errors at some other frequencies (e.g., 9 and 13), but this does not significantly increase  $\lambda_5$ . Accordingly, the operator now has an objective reason to end data collection. At this point the data would appear as illustrated in Figure 2.

There is a significant reduction in time by showing preference for specific frequencies. Assuming the data are statis-

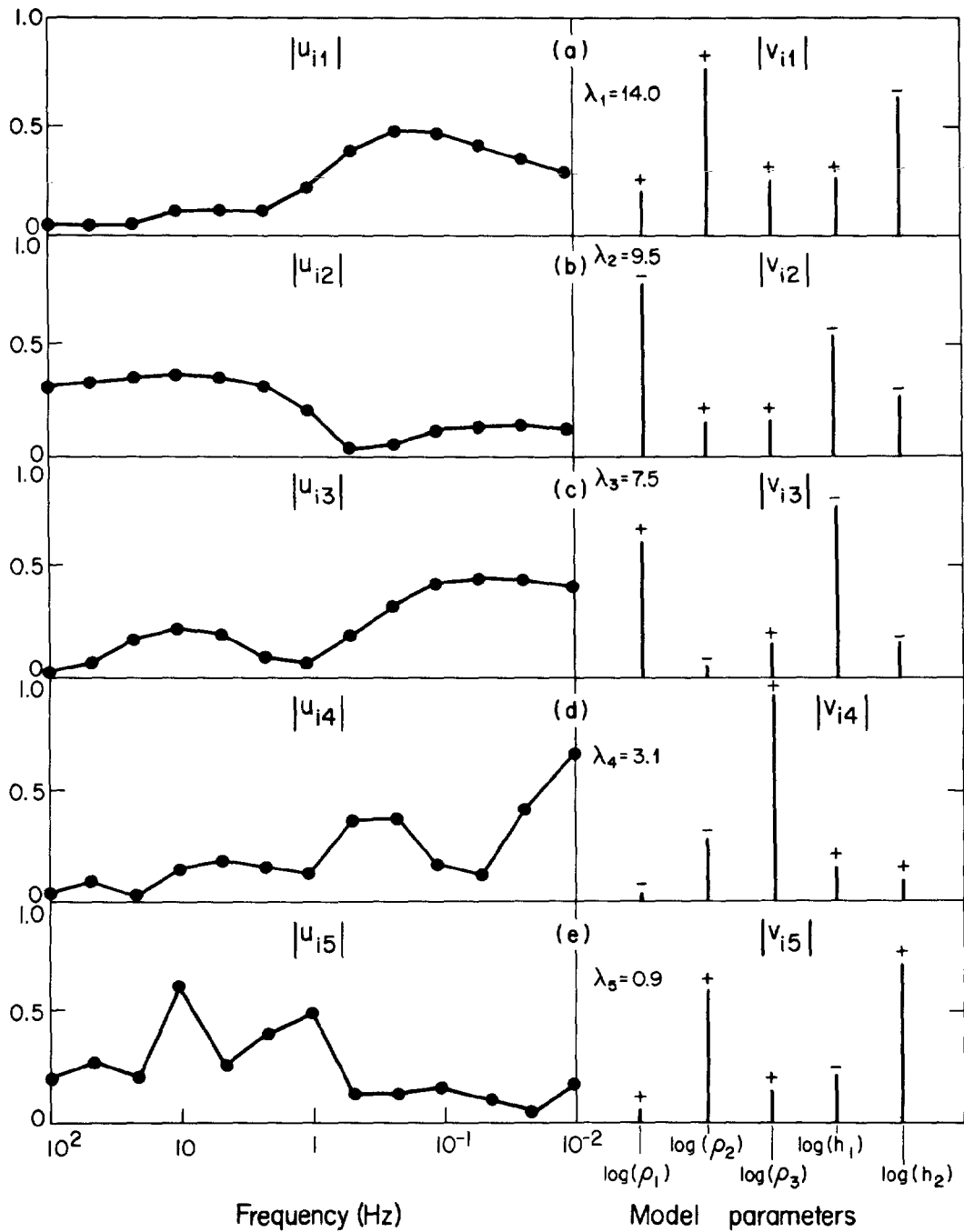


FIG. 3. The SVD analysis of the data illustrated in Figure 2 assuming that all data points had an associated standard error of 25 percent (one-quarter of a decade). The left side of the diagram shows the columns of the  $\mathbf{U}$  matrix (absolute values only), while the right side shows the columns of the  $\mathbf{V}$  matrix, with the associated singular value. The signs above the entries for the  $\mathbf{V}$  matrix indicate the sign of that particular entry. (a) is the best resolved eigenparameter ( $S_2$ ) with  $\lambda_1 = 14.0$  and its eigendata; (e) is the worst resolved eigenparameter ( $T_2$ ) with  $\lambda_5 = 0.9$ . Note that (e) is the same as Figure 4a.

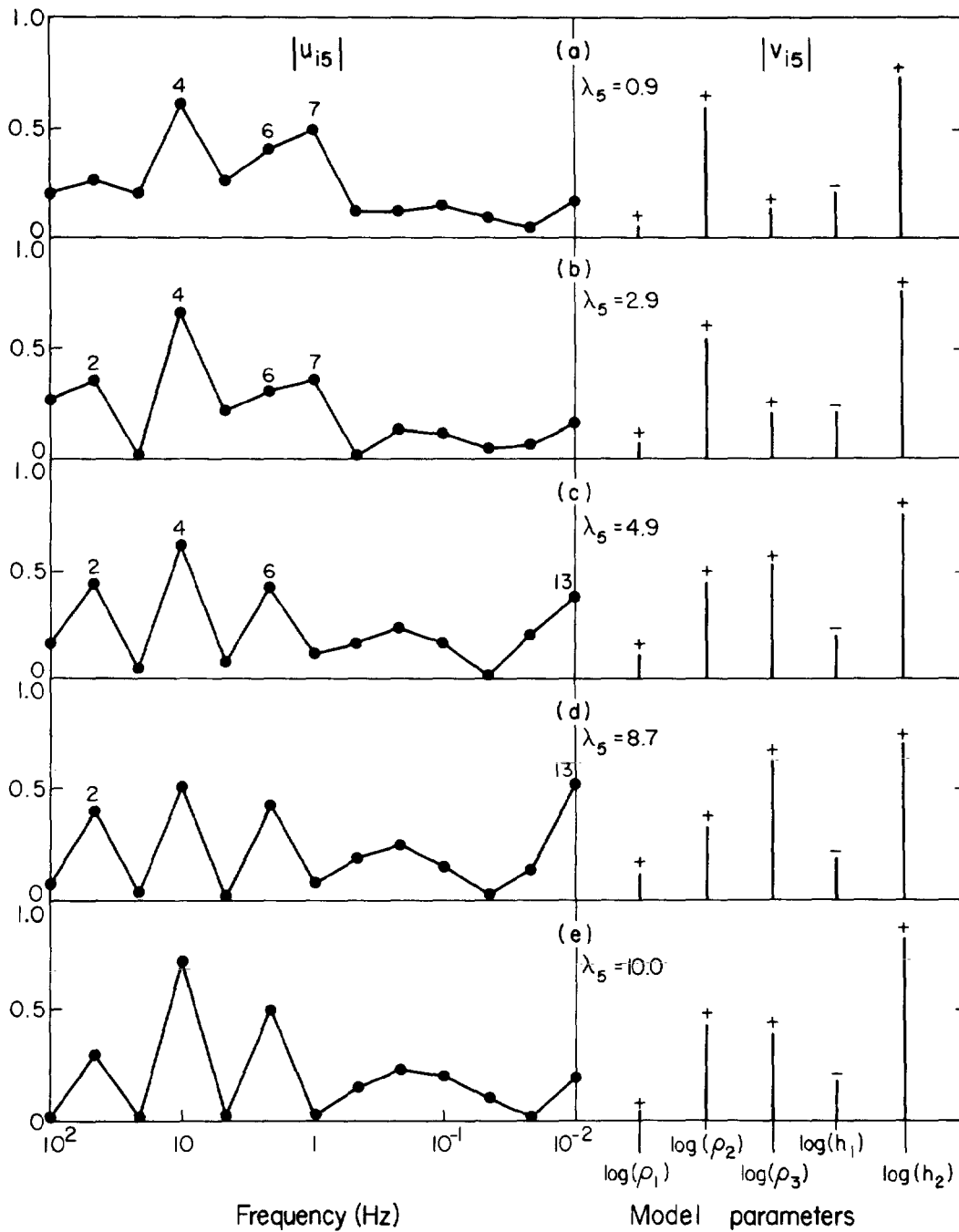


FIG. 4. The last columns of the  $\mathbf{U}$  and  $\mathbf{V}$  matrices at different stages of data acquisition. The worst resolved eigenparameter at each stage is inferred from the contributions to  $v_5$  from each model parameter (the sign above the vertical bars indicates the sign of the contribution). The singular value at each stage is shown by  $\lambda_5$ . The frequencies of most importance for  $v_5$  are denoted by their number. (a) is with all data having 25 percent standard error, and is the starting point for the data-adaptive scheme; (e) is the end point with the data as illustrated in Figure 2.

tically distributed such that doubling the observations reduces the standard error by 1.414 (i.e.,  $\sqrt{2}$ ) and after  $x$  units of time data at one frequency have 25 percent standard error, then to reduce the error at all 13 frequencies from 25 to 3 percent requires  $13 \times (3)^2 x = 117x$  time units. For the example discussed above, only  $35x$  time units are required (reducing frequencies 2, 4, and 6 from 25 to 3 percent, and frequencies 7 and 13 from 25 to 6 percent), a saving of two-thirds of the time required for data acquisition.

FIELD EXAMPLE

An example of the application of the proposed data-adaptive technique to real data is taken from the recent MT survey of Prince Edward Island by Jones and Garland (1985) for geothermal energy resources, using Earth Physics Branch's PHOENIX real-time MT system. For frequencies in the HI-RANGE mode (1-384 Hz), at any one moment in time the system concentrates data collection on two particular frequencies by using narrow band-pass filters. In LO-RANGE mode at the lower frequencies (1-2 000 s period), the data are wide-band collected and are analyzed in real time by a cascade decimation scheme (Wight et al., 1977). Accordingly, at the higher frequencies, the system is perfectly suited for application of this data-adaptive technique.

At an early stage in HI-RANGE (after averaging 50 harmonics) during recording at one particular site on the eastern half of the island, the MT apparent resistivity responses for the high-frequency data were as illustrated in Figure 5 (data illustrated by  $\pm 1$  standard deviation error bars). These data were polynomially smoothed (smoothed data points illustrated as open circles on Figure 5), and the data evaluation software was executed. The "first approximation" model was of a three-layer earth with parameters and theoretical response (solid circles) as illustrated in Figure 5. The worst resolved model eigenparameter was  $\rho_3$ , the resistivity of the half-space, with a standard error of greater than 100 percent.

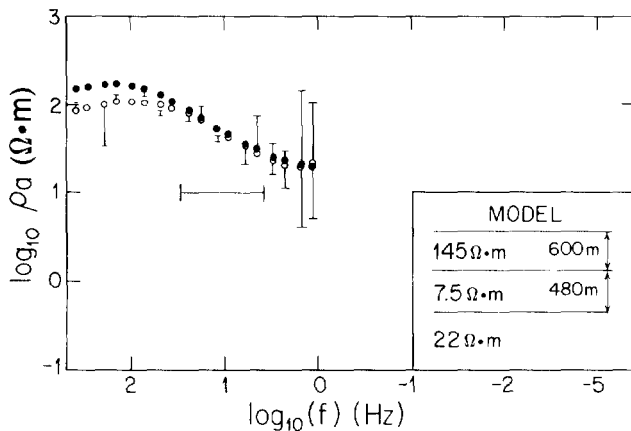


FIG. 5. The apparent resistivity data (plus or minus one standard error) at an early stage of data acquisition for the field survey. (The actual data are not shown if they and their errors lie within the smoothed data, as shown by open circles.) The first-approximation inverse of the smoothed data is illustrated with its theoretical response (solid circles). The frequencies that warrant attention to improve the resolution of the worst resolved eigenparameter (in this case  $\rho_3$ ) are within the horizontal bar.

To increase resolution of  $\rho_3$ , the frequencies within the marked band on Figure 5 warranted attention. Note that at this stage reducing the standard errors of the lowest two frequencies (those with the largest error bars in Figure 5) does not significantly improve the resolution of  $\rho_3$  compared to reducing the standard errors of the frequencies in the marked band (9 percent contribution to the resolution of  $\rho_3$  compared to 53 percent). After each cycle of data acquisition, the recommendations of the data evaluation scheme were followed until the data were as illustrated in Figure 6. At this point, the first-approximation model was of two layers with  $\rho_2$  as the worst-resolved model eigenparameter with an associated standard error of 23 percent. To improve accuracy, the frequencies within the band shown in Figure 6 required more precise data. This was not considered possible; and accordingly the system was switched to LO-RANGE cascade decimation mode.

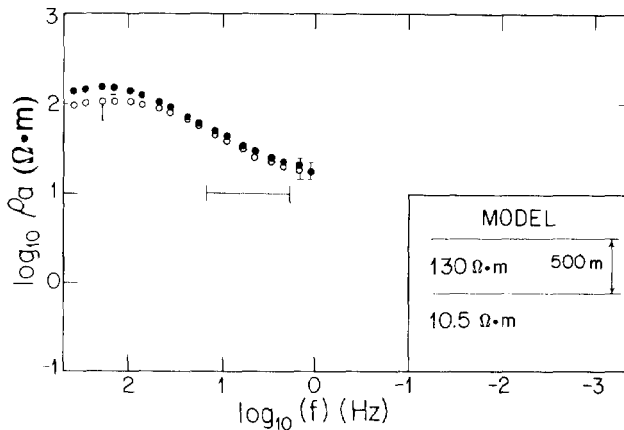


FIG. 6. The apparent resistivity curve at the conclusion of data acquisition in HI-RANGE (1-384 Hz), with the smoothed curve (open circles) and the theoretical response of the first-approximation model shown (solid circles). The data at the frequencies within the horizontal bar would have to have their errors reduced to resolve  $\rho_2$  better (the worst resolved eigenparameter).

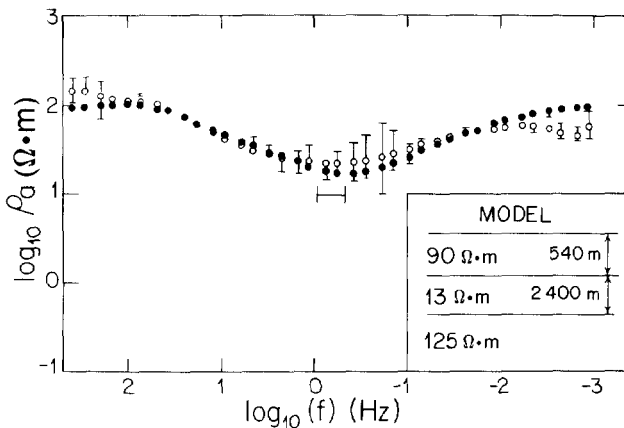


FIG. 7. The apparent resistivity curve at the conclusion of data acquisition, together with the smoothed curve (open circles) and the theoretical response of the first-approximation model shown (solid circles). The data at the two frequencies within the horizontal bar would have to have their errors reduced to improve the resolution of  $T_2$ , i.e.,  $\rho_2 h_2$  (the worst resolved eigenparameter).

After recording in LO-RANGE mode until the data were as illustrated in Figure 7, the data evaluation software indicated that the worst resolved eigenparameter was  $\rho_2 h_2$  (or  $T_2$ ) with a standard error of 31 percent. The most significant improvement in resolution could have been obtained by reducing the standard errors at the two frequencies indicated in Figure 7. Again note that reducing the standard errors of those frequencies with the largest standard errors does not increase the resolution of  $\rho_2 h_2$ , which may mislead an operator into wasting valuable time trying to reduce the standard errors at all frequencies.

At this point it was decided that no significant further improvement could be obtained by continued data acquisition.

### CONCLUSION

The data-adaptive scheme described here statistically analyzes a model that is representative of the conductivity structure beneath a location. The analysis is based on an SVD of the system matrix relating the observations to the model parameters. Such a factoring yields information detailing the worst-resolved eigenparameter of the model, and also the frequencies that require more precise data to improve the resolution of that eigenparameter.

A fairly crude first-approximation scheme, based on the Niblett-Bostick transformation, was used to seek a model that describes the observations. However, the scheme presented could be replaced by any scheme thought to be superior, provided it is fast enough to operate in real time. (The whole data evaluation package written for the PHOENIX system by the authors will execute in real time without endangering the cascade decimation data acquisition in the LO-RANGE mode, provided the number of model layers is less than seven.)

Obviously, the scheme only functions totally correctly at locations where the earth is considered 1-D, e.g., in a sedimentary basin environment. However, in many 2-D situations one of the apparent resistivity curves may be interpreted in a 1-D manner (Jones and Hutton, 1979). The choice of which of the two curves to take requires a priori knowledge of the region, and hence this scheme may be useful on follow-up surveys. For 3-D structure, neither of the two responses may be interpreted in a 1-D manner, and accordingly this data evaluation scheme should not be used.

### ACKNOWLEDGMENTS

The authors express appreciation to the personnel of Earth Physics Branch and Bob Lo of Toronto who aided data acquisition on Prince Edward Island. They are also indebted to Professor Chuck Young of Michigan Technological University for loan of extra field sensors that enabled remote-

reference data processing. The comments of the reviewers (K. Vozoff and an unknown reviewer) are greatly appreciated and improved this manuscript.

Contribution no. 1188 of the Earth Physics Branch.

### REFERENCES

- Bentley, C. R., 1973, Error estimation in two-dimensional magnetotelluric analyses: *Phys. Earth Plan. Int.*, **7**, 423-430.
- Bostick, F. X., 1977, A simple almost exact method of MT analysis, in Workshop on electrical methods in geothermal exploration: U.S. Geol. Surv., Contract No. 14080001-8-359.
- Cavaliere, T., and Jones, A. G., 1984, On the identification of a transition zone in electrical conductivity between the lithosphere and asthenosphere: A plea for more precise phase data: *J. Geophys.*, **55**, 23-30.
- Edwards, R. N., Bailey, R. C., and Garland, G. D., 1981, Conductivity anomalies: Lower crust or asthenosphere?: *Phys. Earth Plan. Int.*, **25**, 263-272.
- Fischer, G., Schnegg, P.-A., Peguiron, M., and LeQuang, B. V., 1981, An analytical one-dimension magnetotelluric inversion scheme: *Geophys. J. Roy. Astr. Soc.*, **67**, 257-278.
- Fournier, H. G., and Febrer, J., 1976, Gaussian character of the distribution of magnetotelluric results working in log-space: *Phys. Earth Plan. Int.*, **12**, 359-364.
- Ilkiskik, O. M., and Jones, A. G., 1984, Statistical evaluation of MT and AMT methods applied to a basalt-covered area in southeastern Anatolia, Turkey: *Geophys. Prosp.*, **32**, 706-724.
- Jones, A. G., 1982, On the electrical crust-mantle structure in Fennoscandia: No Moho, and the asthenosphere revealed?: *Geophys. J. Roy. Astr. Soc.*, **68**, 371-388.
- 1983, On the equivalence of the "Niblett" and "Bostick" transformations in the magnetotelluric method: *J. Geophys.*, **53**, 72-73.
- Jones, A. G., and Garland, G. D., 1985, Preliminary interpretation of the upper crustal structure beneath Prince Edward Island: *Annal. Geophys.*, in press.
- Jones, A. G., and Hutton, R., 1979, A multi-station magnetotelluric study in southern Scotland—I. Fieldwork, data analysis and results: *Geophys. J. Roy. Astr. Soc.*, **56**, 329-349.
- Jupp, D. L. B., and Vozoff, K., 1975, Stable iterative methods for the inversion of geophysical data: *Geophys. J. Roy. Astr. Soc.*, **42**, 957-976.
- 1977a, Two-dimensional magnetotelluric inversion: *Geophys. J. Roy. Astr. Soc.*, **50**, 333-352.
- 1977b, Resolving anisotropy in layered media by joint inversion: *Geophys. Prosp.*, **25**, 460-470.
- Lanczos, C., 1961, Linear differential operators: D. Van Nostrand Co.
- Lawson, C. L., and Hanson, R. J., 1974, Solving least-squares problems: Prentice-Hall, Inc.
- Maillet, R., 1947, The fundamental equations of electrical prospecting: *Geophysics*, **12**, 529-556.
- Niblett, E. R., and Sayn-Wittgenstein, C., 1960, Variation of the electrical conductivity with depth by magnetotelluric method: *Geophysics*, **25**, 998-1008.
- Vozoff, K., and Jupp, D. L. B., 1975, Joint inversion of geophysical data: *Geophys. J. Roy. Astr. Soc.*, **42**, 977-991.
- 1977, Effective search for a buried layer: An approach to experimental design in geophysics: *Austral. Soc. Expl. Geophys.*, **8**, 6-15.
- Wiggins, R. A., 1972, The general linear inverse problem: Implications of surface waves and free oscillations for Earth structure: *Rev. Geophys.*, *Space Phys.*, **10**, 251-285.
- Wight, D. E., Bostick, F. X., Jr., and Smith, H. W., 1977, Real-time Fourier transformation of magnetotelluric data: *Electr. Geophys. Res. Lab. Rep.*, Univ. Texas at Austin.